Simulating Lumbar Spine Motion: Parameter Estimation for Realistic Modeling

Ahmed Sameh

Computer Science Department, the American University in Cairo. 113 Kaser Al Aini Street, Egypt

Abstract. In this paper a general framework for modeling and simulation of the dynamic, three-dimensional motion response of the human lumbar-spine is presented. Lumbar vertebrae were modeled as rigid bodies and all other flexible joint structures (i.e. ligaments, cartilage, muscles, and tendons) were modeled collectively as massless springs and dampers. Coupling coefficients, providing additional constraints, were incorporated in the model. Unknown model coefficients (nominally spring, damping and coupling coefficients) were automatically determined by systematically matching the model predictions to spine displacement-time data. A robust parameter optimization module (Monte Carlo routine and genetic algorithm) was developed for this purpose.

1 Introduction

The human spine has over 100 articulating joints, which are comprised of "rigid" structures (vertebral bodies) and "flexible joint structures" (i.e. ligaments, cartilage. muscles, and tendons) that permit complex and coupled motion patterns. Loads and daily activities impart demands on the spine that often lead to spinal dysfunction and pain, particularly in the lumbar region where loads and moments are generally the highest. Development of reliable methods and tools to quantify the force-induced displacement response of the spine is an important first step toward understanding and predicting vertebral mechanical behavior. Without resorting to invasive spine measurements techniques, precise assessment of clinically relevant variables, such as vertebral and intervertebral displacements and stiffness, is very difficult to obtain (Colloca et al., 2001). Mathematical models are therefore often used to quantify the forces and moments acting on the spine. The mechanical response of the spine to externally applied static and dynamic forces is dependent on the complex interaction between the flexible joint structures (FJS) and rigid structures that comprise the function spinal unit. The lumbar spine vertebrae were modeled as five rigid bodies representing vertebral segments L1 to L5. Each vertebra was treated as a rigid-body mass possessing six displacement degrees of freedom: three components of translation and three components of rotation. All other flexible joint structures (i.e. ligaments, disc, muscles, tendons, and cartilage) or FJS were modeled as massless springs (elastic elements) and dampers (viscous elements) constraining the motion of the vertebrae in the six degrees of freedom. The flexible connections to the upper and lower part of the spine (thorax and pelvis) were also represented as spring-dashpot mechanical elements. Figure 1 shows a schematic diagram of the mechanical equivalence of the lumbar spine and the coordinate system.

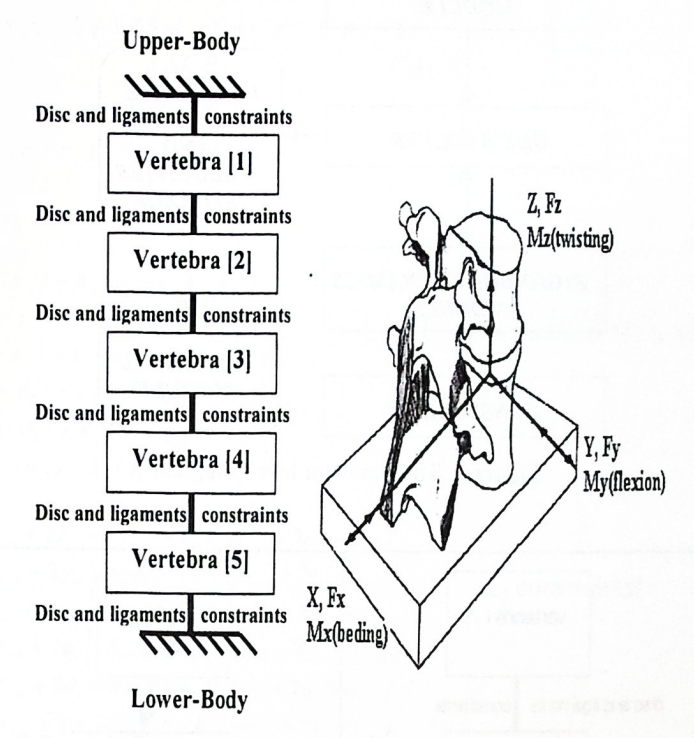


Figure 1. Schematic diagram of the mechanical equivalence of the lumbar spine with description of the coordinate System

Table 1. Vertebrae mass and inert	ia properties
-----------------------------------	---------------

Property	Lı	L ₂	L ₃	L ₄	L ₅
Mass (kg)	0.17	0.17	0.114	0.114	0.114
$I_{xx} (10^{-6}) \text{ kgm}^2$	26.7	24.5	16.5	14.8	22.5
$I_{yy} (10^{-6}) \text{ kgm}^2$	34.2	31	17.4	20.4	31
I_{zz} (10 ⁻⁶) kgm ²	36.8	36	22.2	26.5	40.3
I_{xz} (10 ⁻⁶) kgm ²	-7.8	-6.9	-2.8	1.4	2.12

Two solvers are implemented in the simulator. For parameter estimations, a first order finite difference procedure is implemented to speed up calculations. For the simulator a fourth order Runge-Kutta procedure is implemented for high accuracy.

$$F_{x,i} - m_i g \sin(\theta_i) = m_i (u_i^k + q_i w_i - r_i v_i)$$

$$F_{y,i} + m_i g \cos(\theta_i) \sin(\phi_i) = m_i (u_i^k + r_i u_i - p_i w_i)$$

$$F_{-i} + m_i g \cos(\theta_i) \sin(\phi_i) = m_i (u_i^k + p_i v_i - q_i u_i)$$

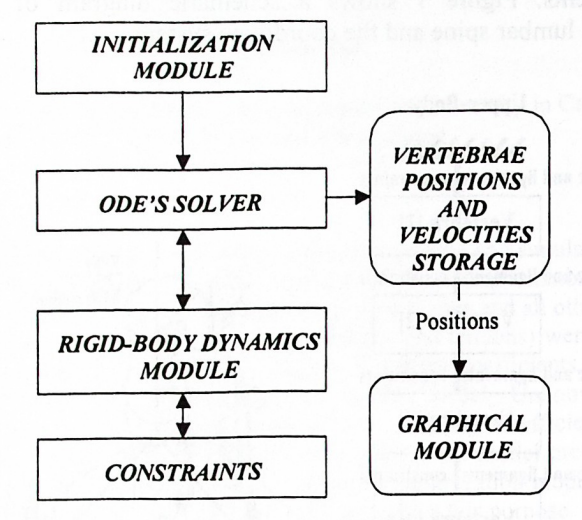


Figure 2. The simulator block diagram

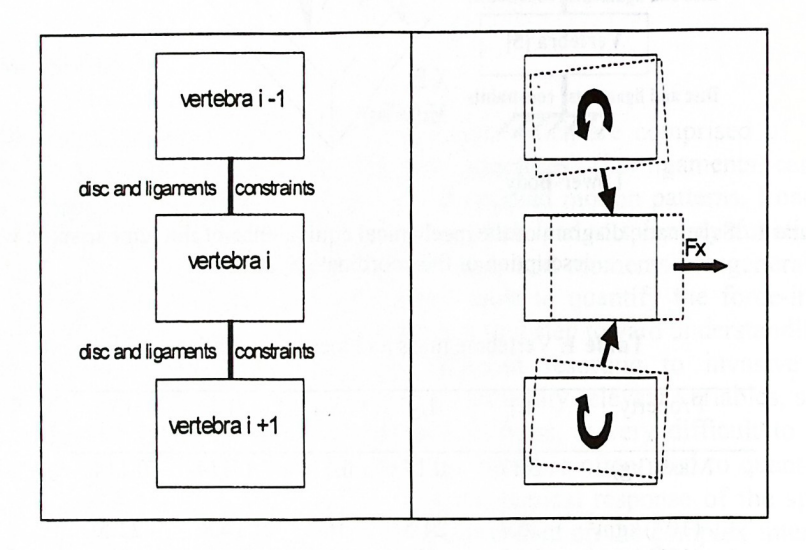


Figure 3. Coupling motion

$$\begin{split} M_{xi} &= (I_{x})_{i} \not \otimes_{i} - (I_{xz})_{i} \not \otimes_{i} + q_{i} r_{i} (I_{z} - I_{y})_{i} - (I_{xz})_{i} p_{i} q_{i} \\ M_{yi} &= (I_{y})_{i} \not \otimes_{i} + q_{i} r_{i} (I_{x} - I_{z})_{i} + (I_{xz})_{i} (p_{i}^{2} - r_{i}^{2}) \\ M_{zi} &= n (I_{xz})_{i} \not \otimes_{i} + (I_{z})_{i} \not \otimes_{i} + q_{i} p_{i} (I_{y} - I_{z})_{i} - (I_{xz})_{i} r_{i} q_{i} \\ \not \otimes_{i}^{2} &= q_{i} \cos(\phi_{i}) - r_{i} \sin(\phi_{i}) \\ \not \otimes_{i}^{2} &= p_{i} + q_{i} \sin(\phi_{i}) \tan(\theta_{i}) - r_{i} \cos(\phi_{i}) \tan(\theta_{i}) \\ y \not \otimes_{i}^{2} &= (q_{i} \sin(\phi_{i}) - r_{i} \cos(\phi_{i})) \sec(\theta_{i}) \end{split}$$

$$(1)$$

$$\begin{bmatrix} \frac{dx}{dt} \\ \frac{dy}{dt} \\ \frac{dz}{dt} \end{bmatrix}_{i} = \begin{bmatrix} C\theta_{i}C\psi_{i} & S\phi_{i}S\theta_{i}C\psi_{i} - C\phi_{i}S\psi_{i} & C\phi_{i}S\theta_{i}C\psi_{i} + S\phi_{i}S\psi_{i} \\ C\theta_{i}S\psi_{i} & S\phi_{i}S\theta_{i}S\psi_{i} + C\phi_{i}C\psi_{i} & C\phi_{i}S\theta_{i}S\psi_{i} - S\phi_{i}C\psi_{i} \\ -S\theta_{i} & S\phi_{i}C\theta_{i} & C\phi_{i}C\theta_{i} \end{bmatrix} \begin{bmatrix} u \\ v \\ w \end{bmatrix}$$

where $Cx_i \equiv cos(x_i)$, $Sx_i \equiv sin(x_i)$

L₁ constraints:

$$F_{v} = -k_{v}(x_{1} - x_{2}) - k_{n}(u_{1} - u_{2}) - k_{x_{1}}x_{1}$$

$$F_{v} = -k_{v}(y_{1} - y_{2}) - k_{v}(v_{1} - v_{2}) - k_{y_{1}}y_{1}$$

$$F_{z} = -k_{z}(z_{1} - z_{2}) - k_{w}(w_{1} - w_{2}) - k_{z_{1}}z_{1}$$

$$M_{x} = -k_{\phi}(\phi_{1} - \phi_{2}) - k_{p}(p_{1} - p_{2}) - k_{\phi}\phi_{1}$$

$$M_{y} = -k_{\theta}(\theta_{1} - \theta_{2}) - k_{q}(q_{1} - q_{2}) - k_{\eta}\theta_{1}$$

$$M_{z} = -k_{w}(\psi_{1} - \psi_{2}) - k_{r}(r_{1} - r_{2}) - k_{w}\psi_{1}$$

 L_2 to L_4 constraints (i=2, 3, 4):

$$\begin{split} F_x &= -k_x \left(-x_{i-1} + 2x_i - x_{i+1} \right) - k_y \left(-u_{i-1} + 2u_i - u_{i+1} \right) \\ F_v &= -k_y \left(-y_{i-1} + 2y_i - y_{i+1} \right) - k_y \left(-v_{i-1} + 2v_i - v_{i+1} \right) \\ F_z &= -k_z \left(-z_{i-1} + 2z_i - z_{i+1} \right) - k_y \left(-w_{i-1} + 2w_i - w_{i+1} \right) \\ M_x &= -k_\phi \left(-\phi_{i-1} + 2\phi_i - \phi_{i+1} \right) - k_y \left(-p_{i-1} + 2p_i - p_{i+1} \right) \\ M_y &= -k_y \left(-\theta_{i-1} + 2\theta_i - \theta_{i+1} \right) - k_y \left(-q_{i-1} + 2q_i - q_{i+1} \right) \\ M_z &= -k_y \left(-\psi_{i-1} + 2\psi_i - \psi_{i+1} \right) - k_z \left(-r_{i-1} + 2r_i - r_{i+1} \right) \end{split}$$

L₅ constraints:

$$F_{x} = -k_{x}(x_{5} - x_{4}) - k_{y}(u_{5} - u_{4}) - k_{x2}x_{5}$$

$$F_{y} = -k_{y}(y_{5} - y_{4}) - k_{y}(v_{5} - v_{4}) - k_{y2}y_{5}$$

$$F_{z} = -k_{z}(z_{5} - z_{4}) - k_{y}(w_{5} - w_{4}) - k_{z2}z_{5}$$

$$M_{x} = -k_{\theta}(\phi_{5} - \phi_{4}) - k_{p}(p_{5} - p_{4}) - k_{\theta2}\phi_{5}$$

$$M_{y} = -k_{\theta}(\theta_{5} - \theta_{4}) - k_{q}(q_{5} - q_{4}) - k_{\theta2}\theta_{5}$$

$$M_{z} = -k_{y}(\psi_{5} - \psi_{4}) - k_{r}(r_{5} - r_{4}) - k_{y2}\psi_{5}$$
(2)

$$F_{ze1} = -k_{zx} F_{x2} \qquad M_{c1} = -k_{\theta x} F_{x2}$$

$$F_{ze2} = k_{zx} F_{x1} - k_{zx} F_{x3} \qquad M_{c2} = k_{\theta x} F_{x1} - k_{\theta x} F_{x3} \qquad (3a)$$

$$F_{ze3} = k_{zx} F_{x2} - k_{zx} F_{x4} \qquad M_{c3} = k_{\theta x} F_{x2} - k_{\theta x} F_{x4}$$

$$F_{ze4} = k_{zx} F_{x3} - k_{zx} F_{x5} \qquad M_{c4} = k_{\theta x} F_{x3} - k_{\theta x} F_{x5}$$

$$F_{ze5} = k_{zx} F_{x4} \qquad M_{c5} = k_{\theta x} F_{x4}$$

$$F_{ze1} = -k_{zy} F_{y2} \qquad L_{c1} = -k_{yy} F_{y2} \qquad (21a)$$

$$F_{ze1} = -K_{xy}F_{y2}$$

$$F_{ze2} = k_{zy}F_{y1} - k_{zy}F_{y3}$$

$$F_{ze3} = k_{zy}F_{y2} - k_{zy}F_{y4}$$

$$F_{ze4} = k_{zy}F_{y3} - k_{zy}F_{y5}$$

$$L_{e3} = k_{yy}F_{y2} - k_{yy}F_{y4}$$

$$L_{e3} = k_{yy}F_{y2} - k_{yy}F_{y4}$$

$$L_{e4} = k_{yy}F_{y3} - k_{yy}F_{y5}$$

$$L_{e5} = k_{zy}F_{y4}$$

$$L_{e5} = k_{yy}F_{y4}$$
(3b)

The parameter estimation algorithm proceeds as follows:

- 1- Initialize parameters (spring and dashpot coefficients).
- 2- Run the simulator with known input-output data pairs.
- 3- Calculate the simulator output and compare it with the actual spine output and calculate the error function.
- 4- Repeat steps 1-3 through the optimizer to minimize the error function till reaching minimum.
- 5- End.

The optimizer uses a robust optimization procedure based on a Monte Carlo procedure followed by genetic algorithm (GA) detailed in the following section. Parameter estimates for the spring, damper and coupling coefficients are not generally available, or are highly variable. Hence, a Monte Carlo technique (Murray, 1972) was employed to obtain candidate solutions to start a genetic algorithm (GA) (Goldberg, 1989). The Monte Carlo technique implemented in the optimizer is as follows:

- 1- Generate the unknown parameters randomly.
- 2- Substitute into the cost function and calculate the error.
- 3- Repeat step 1 and 2 (n) times.
- 4- Keep the best m trails with the minimum error.
- 5- Pass these trials to the GA algorithm.

The GA proceeds with the initial population taken from the Monte Carlo procedure. The full optimizer block diagram is shown in Figure 4.

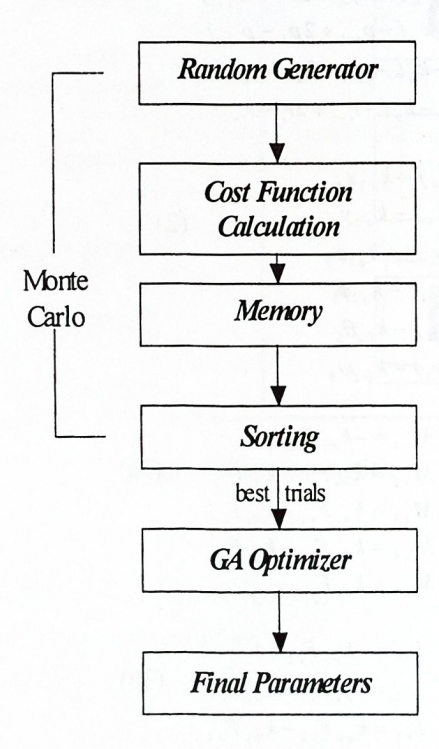


Figure 4. Block diagram of the unknown spring, damper and coupling coefficient parameter estimation procedure

Alternatively, if initial spring, damper and coupling parameters estimates are available, then an optimization technique such as steepest decent is employed. For a single variable, this can be written as

cost function (f) =
$$\int |e(t)| dt$$

where
$$e(t) = V_{exp}(t) - V_{model}(t)$$
,

For multiple variables, such as displacement-time histories for different axes, the total cost function is just the summation of cost function of each variable with weighting constants as follows:

Total cost function (F) =
$$w_1 f_1 + w_2 f_2 + \dots + w_n f_n = w_1 \int |e_1(t)| dt + w_2 \int |e_2(t)| dt + \dots + w_n \int |e_n(t)| dt$$

Six displacement-time histories data represent the posteroanterior (PA or X-axis) displacement, axial (AX or Z-axis) displacement, and flexion extension (FE) rotation (about Y-axis) for the L3 and L3-L4 vertebral segments subjected to an impulsive force of 100 N applied to the L3 vertebra of a 36 year old, 185 cm, 82 kg male volunteer. Displacement-time histories, with equal time steps (0.2 msec.) were obtained from Keller's model (Keller et al., 2002). The cost function is given by

Total cost function (F) =
$$\sum_{i=1}^{6} \varepsilon_i$$

where

$$\varepsilon_1 = \sum |(axial \text{ displacement}_{Keller} - axial \text{ displacement}_{Model})| \text{ for } L_3$$

$$\varepsilon_2 = \sum_{\text{Keller}} |(axial \text{ displacement}_{\text{Keller}} - axial \text{ displacement}_{\text{Model}})| \text{ for } L_4$$

$$\varepsilon_3 = \sum |(PA \text{ displacement}_{\text{Keller}} - PA \text{ displacement}_{\text{Model}})| \text{ for } L_3$$

$$\varepsilon_4 = \sum |(PA \text{ displacement}_{Keller} - PA \text{ displacement}_{Model})| \text{ for } L_4$$

$$\varepsilon_5 = \sum |(FE \text{ displacement}_{Keller} - FE \text{ displacement}_{Model})| \text{ for } L_3$$

$$\varepsilon_6 = \sum |(FE \text{ displacement}_{Keller} - FE \text{ displacement}_{Model})| \text{ for } L_4$$

The cost function is given by

Total cost function (F) =
$$\sum_{i=1}^{3} \varepsilon_{i}$$

where

$$\varepsilon_1 = \sum \left| (axial\ rotation_{Tsung} - axial\ rotation_{Model}) \right|$$
 for L₃

$$\varepsilon_2 = \sum_{\text{constant}} |(lateral \ bending_{\text{Tsung}} - lateral \ bending_{\text{Model}})| \text{ for } L_3$$

$$\varepsilon_3 = \sum \left| (flextion\ extension_{Tsung} - flextion\ extension_{Model}) \right| \text{ for } L_3$$

2 Results

Figure 5 graphically illustrates the experimental (Keller et al., 2002) and parameter optimized axial (AX), transverse (PA), and FE rotation displacement-time histories. Coefficients derived from the impulsive force optimization procedure were used to simulate the PA static and

oscillatory force response (100 N peak amplitude). The model predictions compare favorably with experimental results (Table 2, 3).

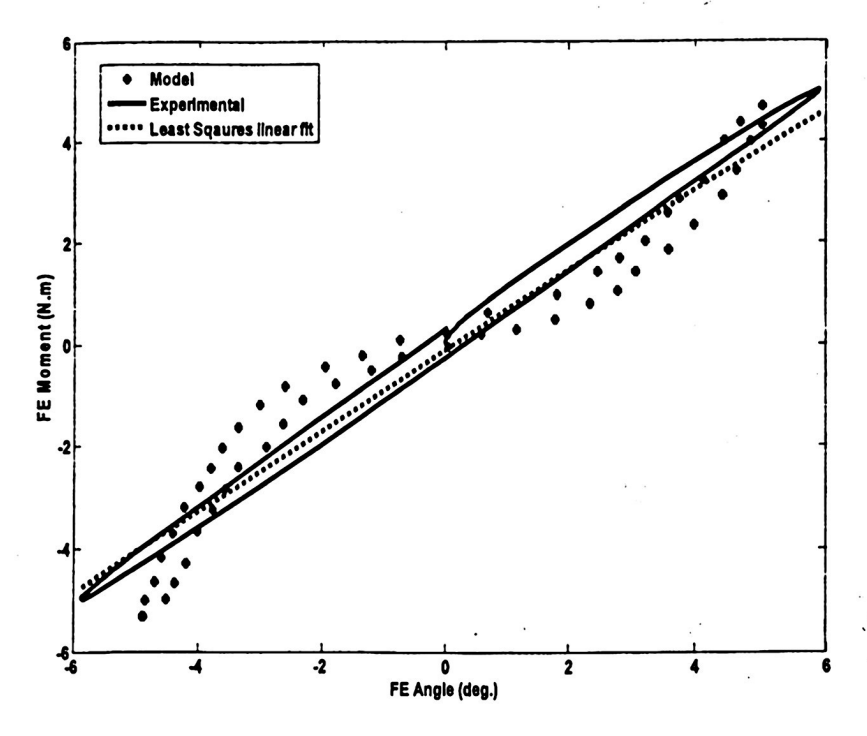


Figure 5. Experimental and parameter optimized axial (AX), transverse (PA), and FE rotation displacement-time histories

Table 2. Peak-to-peak displacements obtained for static PA forces of 100N.

Vertebral	Displacement	Keller's	Spinal	% error
Segment	Axis		Model	
L ₃	PA (mm)	7.97	7.95	0.2
	AX (mm)	0.131	0.137	-1.9
	FE rotation (°)	0.374	0.355	4.99
L_4	PA (mm)	5.42	5.38	0.3
	AX (mm)	0.70	0.759	-8.6
	FE rotation (°)	1.83	2.03	-10.8

	2 Hz		5.2 Hz	
	L,	L3-L4	L,	L3-L4
Keller's data [2]	8.23	2.65	7.67	2.55
Spinal model	7.2	2.3	6.1	2
% error	12.2	13.1	19	21

Table 3. PA Peak-to-peak L₃, L₃-L₄ response sinusoidal force at L₃

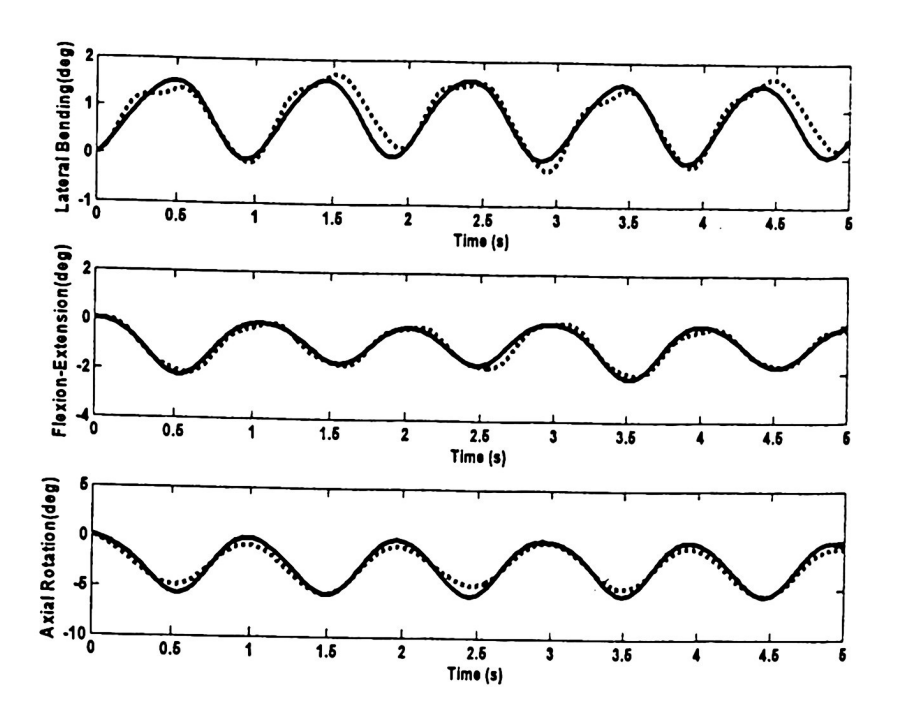
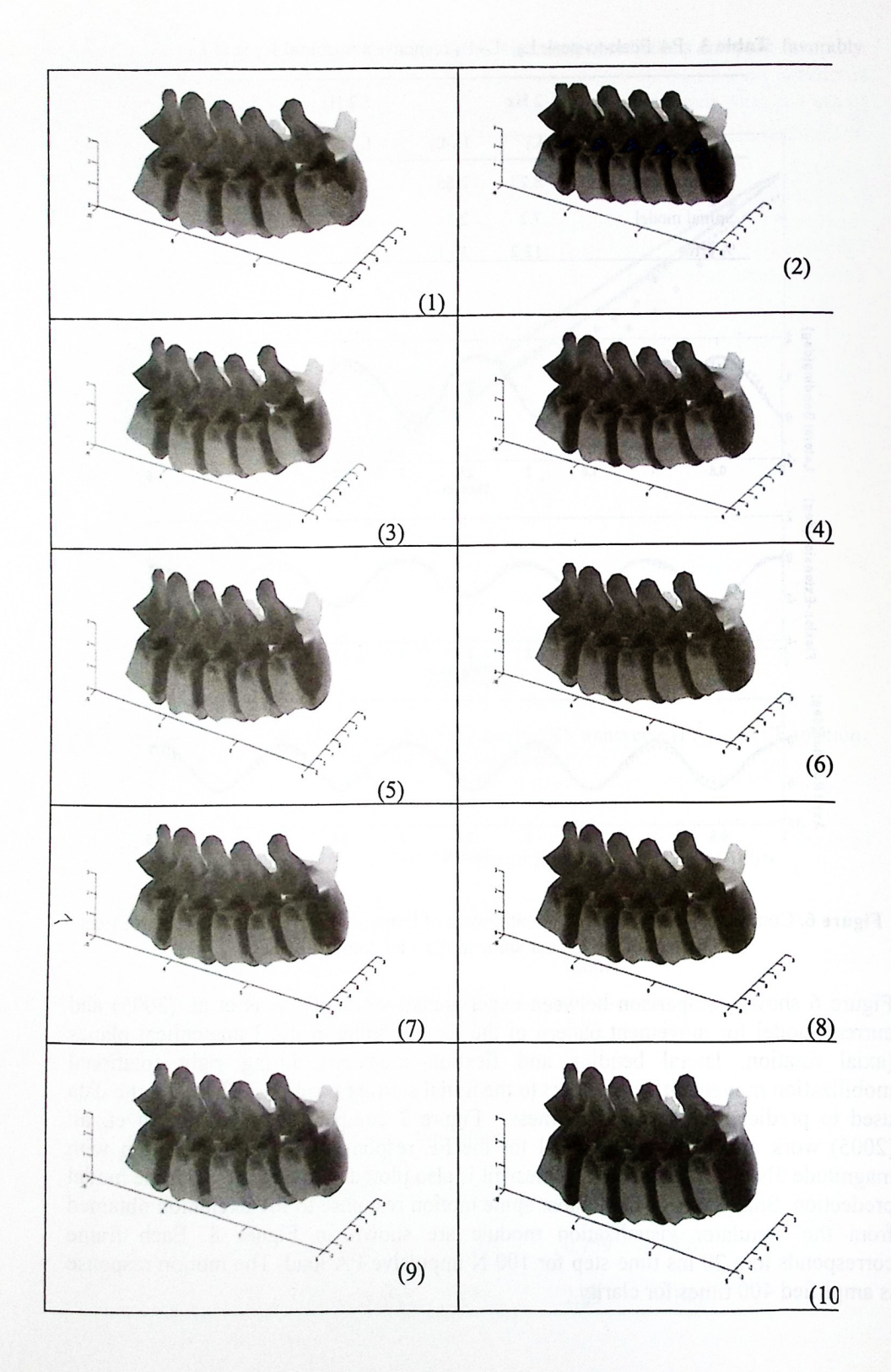


Figure 6. Comparison between experimental work of Evans and current model for movement pattern of the lumbar spine in the 3 anatomical planes

Figure 6 shows comparison between experimental work of Evans et al. (2005) and current model for movement pattern of the lumbar spine in the 3 anatomical planes (axial rotation, lateral bending and flextion-extension) during right rotational mobilization movement with respect to the initial starting positions. These are the data used to predict the rotational stiffness. Figure 7 compares between Ralph et. al. (2005) work and the current model for the FE response for cyclic excitation with magnitude 5N.m. A least-squares linear fit is also ploted which agrees with the model predection. Snap shots of the lumbar spine motion response to PA excitation obtained from the simulator visualization module are shown in Figure 8. Each frame corresponds to a 20 ms time step for 100 N impulsive PA load. The motion response is amplified 400 times for clarity.



3 Conclusions

The semi-analytical lumbar spine dynamic motion simulator was tested using PA, FE and axial segmental and intersegmental displacement-time data obtained from impulsive force experiments and angular movement pattern from rotational mobilization. Parameter optimized model simulations showed good agreement with the test data, and subsequent independent validation of the static and oscillatory displacement response demonstrated that impulsive force and rotational mobilization test data can be used to predict the lumbar spine motion response during other types of loading conditions. Lumped parameter models, therefore, provide an efficient and effective method to determine the vertebral and/or intervertebral displacement-time history response of the lumbar spine to static, dynamic and impact forces.

References

- 1. Tony S. Keller, Christopher J. Colloca, Jean-Guy Beliveau, 2002. Force-deformation response of the lumbar spine: a sagittal plane model of posteroanterior manipulation and mobilization, *Clinical Biomechanics*, 17(3), 185-196.
- 2. Lee RYW, Evans JH., 1994. Towards a better understanding of posteroanterior mobilization. Physiotherapy 80, 68-73.
- 3. Lee M., Kelly DW, and Steven, 1995. A model of spine, ribcage, and pelvic responses to a specific lumbar manipulative force in relaxed subjects, Journal of Biomechanics 28(11): 1403-1408.
- Tsung Bonnie Y. S., Evans JH, Pin Tong, Lee Raymond Y. W., 2005. Measurement of lumbar spine loads and motions during rotational mobilization, Journal of Manipulative and Physiological Therapeutics, vol. 28, no4, pp. 238-244
- 5. Amed A. Shabana, 2001. Computational Dynamics. John Wiley and Sons, pp. 423-427.
- 6. Robert C. Nelson, 1998. Flight stability and automatic control. McGraw Hill, pp.
- 7. Christian P. Robert, George Casella, 2005. Monte Carlo Statistical Methods. Springer. pp. 157-203.
- 8. D. Goldberg, 1989. Genetic Algorithms in Search, Optimization and Machine Learning. Addison-Wesley, Boston, MA. pp. 106-120.